Study on Soil Water Characteristics of Black Soil, Northeast China

Haiqiang Jiang [1], Fujun Niu [2)], Heng Zhang [3], Enliang Wang [4], Qinguo Ma [5] and Jiehui Xie [6]*

[1] Doctor, South China Institution of Geotechnical Engineering, School of Civil Engineering and Transportation, South China University of Technology, Guangzhou 510641, China. E-Mail: hqiangjiang@126.com
2) Professor, South China Institution of Geotechnical Engineering, School of Civil Engineering and Transportation, South China University of Technology Guangzhou 510641, China.
* Corresponding Author. E- Mail: niufj@scut.edu.cn
[3] Doctor, South China Institution of Geotechnical Engineering, School of Civil Engineering and Transportation, South China University of Technology, Guangzhou 510641, China. E- Mail: 596045638 @qq.com
[4] Professor, School of Water Conservancy and Civil Engineering, Northeast Agricultural University, Harbin 150030, China. E-Mail: wel@neau.edu.cn
[5] Assistant Professor, South China Institution of Geotechnical Engineering, School of Civil Engineering and Transportation, South China University of Technology, Guangzhou 510641, China. E-Mail: Maqg@scut.edu.cn
[6] Doctor, South China Institution of Geotechnical Engineering, School of Civil Engineering and Transportation, South China University of Technology, Guangzhou 510641, China E-Mail: 402265642@qq.com.

ABSTRACT

Black soil has strong swell-shrink characteristics due to the change of water content. Permeability and fractal behavior can be reflected by soil water characteristic curve (SWCC). Although many relevant models can calculate the SWCC, the applicability of these models on black soil is unclear. In addition, the prediction of the SWCC is complicated, as the necessary parameters are difficult and time-consuming to measure. In this context, a series of experiments on the SWCC of black soil was conducted in the laboratory. Based on the results and analysis, conclusions were drawn as follows: The pore fractal dimension is strongly correlated with dry density; that is, the larger the dry density is, the greater the fractal dimension becomes. The permeability coefficient decreases with the increasing of the matric suction. The three commonly SWCC models (Fredlund (1994)**,** Van Genuchten (1980) and Gardner (1958)) are appropriate for predicting the SWCC of black soil. Moreover, the optimized van Genuchten model can improve the accuracy of prediction by replacing the model parameters with the formula of dry density. Compared with the van Genuchten model, the absolute value of relative error decreased from 4.50% to 3.75% after optimization.

INTRODUCTION

Black soil is defined as the soil which contains organic matter content ranging from 3% to 5% and with swell-shrink and disturbance properties (Dong et al., 2019). It accounts for 1.02×10^6 km² in the northeast of China and it's widely distributed in Sonnen Plain (Zheng et al., 2018), which is a main agricultural region in China. In recent years, with land reclamation, the black soil region always appears subject to soil erosion and hardening, which are harmful to the agricultural

production and lead to the loss of soil fertility. Similarly, due to swell-shrink characteristics of the soil and the freezing-thawing action, local engineering constructions are facing big challenges, such as channel crack, slope failure and distortion (Bao et al., 2006; Omer Muhie Eldeen Taha and Moh'd Raihan Taha, 2015).

The properties of black soil are quite different from those of other soils because of unique composition and geographical environment. The SWCC is an important tool to understand the properties of soils. It represents the relationship between matric suction and water content. Meanwhile, the energy and water quality of the soil can be reflected by the SWCC. Many soil properties can be derived from the SWCC, such as permeability

coefficient, shear strength and underground water distribution (Han et al., 2016; Shi et al., 2018; Sahis, 2017). These properties are crucial factors for maintaining security and durability of local engineering.

Previously, the commonly used tools for measuring the SWCC are: volumetric pressure plate, tension meter, contact filter paper and TDR (Hong et al., 2016). With the development of technology, some scholars have used industrial X-ray computed tomography to acquire the SWCC (Scanziani et al., 2017). This method has advantages over other methods, because it allows to clearly observe the soil microstructure and its quantitative affecting factors. However, every measuring method is only suitable for limited ranges of matric suction. To overcome this deficiency, researchers have investigated SWCC models to get an SWCC efficiently（e.g., the Gardner model (Gardner, 1958), van Genuchten model (van Genuchtten, 1980), Fredlund & Xing model (Fredlund, 1994), Books and Corey model (Corey et al., 1975) and Childs & Collis-Geroge model (Childs et al., 1950). It is recognized that a typical SWCC consists of three distinct characteristic zones, which are the boundary zone, the transitional zone and the residual zone, as sketched in Fig. 1 (Mcqueen et al., 1974; Gao et al., 2017). Generally, the matric suction is very weak in the boundary zone. The initial water content approaches the saturated water content and exhibits a slightly downward tendency with the

increasing of the matric suction. A similar phenomenon is also observed in the residual zone. However, in the transitional zone, the water content decreases rapidly with increasing matric suction. According to the tangent intersection point of the boundary zone, transitional zone and residual zone, the coordinate of air entry value and the residual suction are obtained.

In recent years, numerous experimental works have been carried out on soil SWCC. Besides the soil texture, the SWCC is affected by water content, dry density, grain size and porosity (Sedano et al., 2016; Tao et al., 2017; Arya et al., 2017; Mill, 2002; Philip et al., 1957). Among all of these factors, porosity is the most crucial factor, which significantly affects the soil SWCC (Han et al., 2016). Also, when the matric suction is weak, the volumetric water content increases with dry density, which is opposite when the matric suction is strong (Chen et al., 2017; Minh et al., 2018). Moreover, Arya and Paris (1981) proposed the Paris fractal theory, which is a bridge that connects the microscopic structure and the macroscopic characteristics. Fractal behavior and grain distribution of soils can be calculated on the basis of the fractal theory (Feng et al., 2017; Gao et al., 2018). Furthermore, many researchers studied the SWCC by using the fractal theory at the microscopic level and proposed the relevant models to predict the SWCC of different initial conditions (Tao et al., 2014; Wheatcraft et al., 1988; Alexandra et al., 1998).
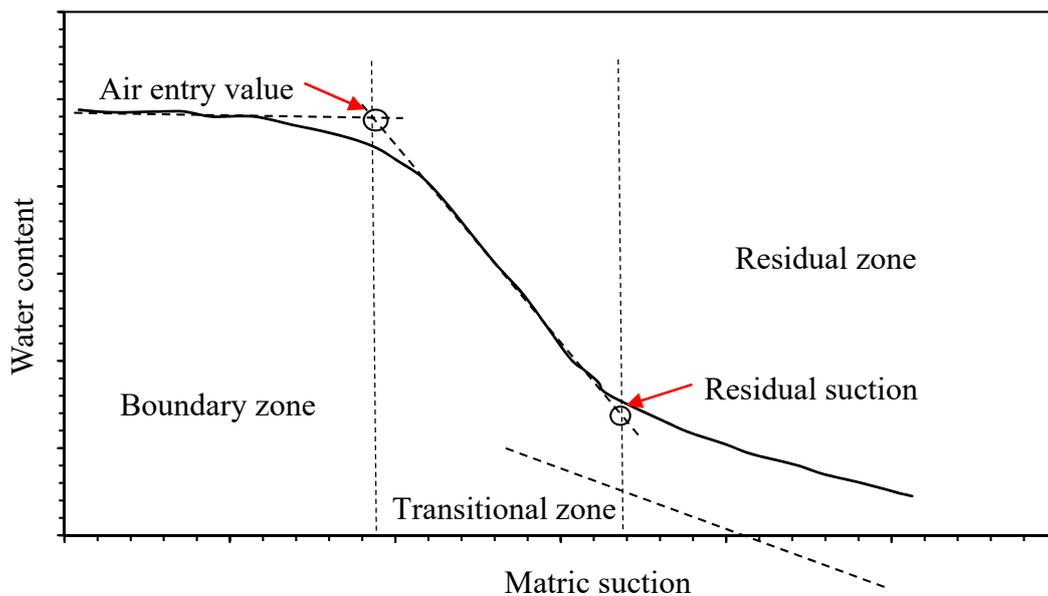

Figure (1): Typical soil water characteristic curve (Gao et al., 2017)

For investigating the SWCC and further understanding the characteristics of the soil, most reference works focused on loess (Jiang et al., 2016), sands (Tabana et al., 2018), silt residual soil (Li et al., 2017; Zhai et al., 2016; Liu et al., 2017) and expansive clay (Elkady et al., 2017; Al-Mahbashi et al., 2016). However, few studies reported on black soil until now and the applicability of the SWCC models to black soil are not clear. In addition, the necessary parameters of commonly used SWCC models are complicated and time-consuming to measure, especially for residual water content. Therefore, in this paper, remolded black soil is selected as the experimental material to solve these problems and acquire more in-depth knowledge about black soil. On the basis of the experimental results, the SWCC of black soil is compared and evaluated for different dry densities, then the performance of the optimized van Genuchten model was verified. Furthermore, the fractal dimension and permeability coefficient of black soil are analyzed.

MATERIALS AND METHODS

Study Area Conditions

In order to obtain the SWCC of black soil, experiments were designed and conducted in Harbin, Heilongjiang Province, as shown in Fig.2. The study area is within plain topography and semi-arid region, where seasonally frozen soil and black soil are extensively distributed all over there. The freezing period is longer than the thawing period. The lowest temperature here is about -40 ℃ in winter and the total annual precipitation is 537.9 mm based on the meteorological records, as shown in Fig.3.

The soil was excavated from depths beneath the ground surface ranging between 20 cm and 80 cm. Laboratory geotechnical tests showed that the specific gravity of solid particles is 2.69. The maximum dry density is 1.72 g cm^{-3} and the plastic limit is 23%.
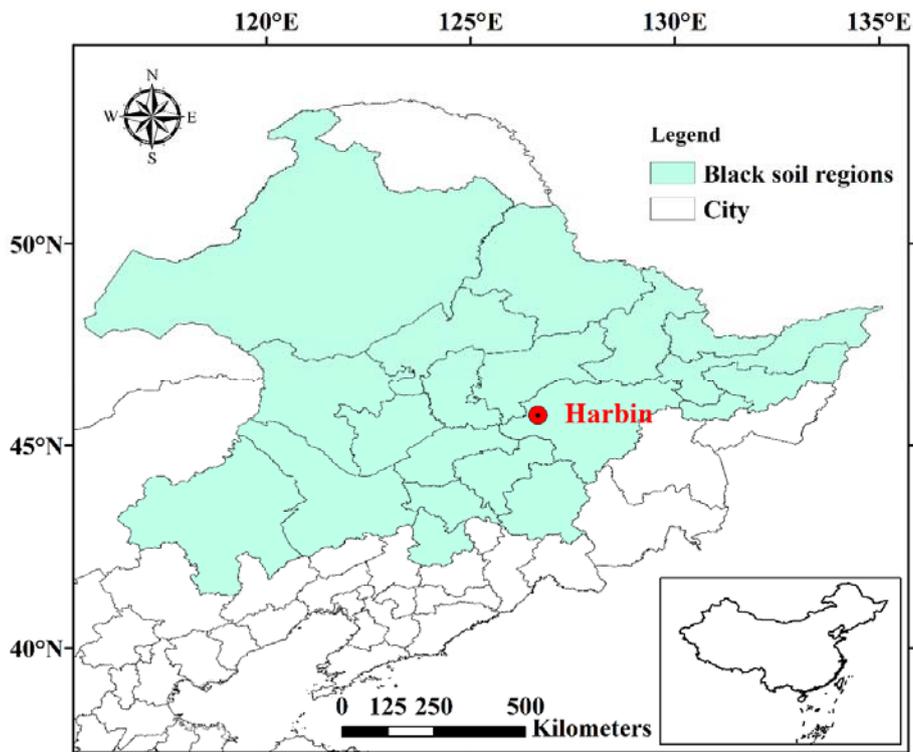

Figure (2): Distribution of black soil regions in China and the studied area
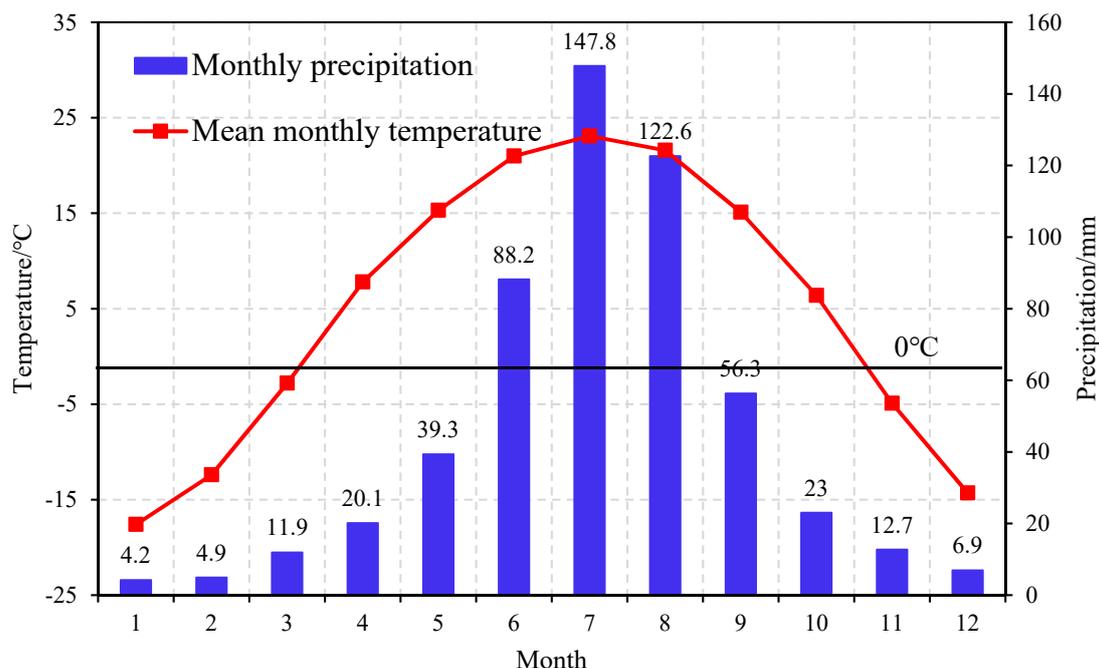
**Figure (3): Mean monthly air temperature and precipitation in Harbin city from 2012 to 2018
(CMA, 2018)**

Experimental Methods

Firstly, the soil was sifted through 2-mm sieve, then the mass water content was measured after drying for 24 hours at 105 °C. The samples were compacted in a total of 5 layers. Dry density was 1.40 g cm⁻³, 1.45 g cm⁻³, 1.55 g cm⁻³, 1.65 g cm⁻³ and 1.70 g cm⁻³, respectively. Four samples were necessary at the same dry density, two of which (S1, S2) were used for determining the saturated permeability coefficient θ_s and residual water content θ_r, respectively. The other two samples were considered as the experimental sample (S3) and the alternative sample (S4).

Secondly, the saturated mass permeability coefficient (k_s) and the residual water content (θ_r) were determined, respectively. According to the Chinese standard for soil test method (GBT50123-2019), the procedure followed is as follows.

(1) The samples were weighed after maintaining them for 21d at a temperature of 20°C and relative humidity of 45 %, then the samples were weighed again after drying for 24 hours at 105°C to obtain θ_r.

(2) The saturated permeability coefficient (k_s) was measured by the TST-55 permeameter at the environmental temperature of 20°C. The variable head method was adopted.

The SWCC was determined by the pressure-membrane measuring instrument. The measurement steps are as follows.

(1) At first, the samples were saturated, then the sample and the high inlet clay plate were placed into the pressure vessel and connected to the external drainage pipe.

(2) After the sample was weighed, it was put on the clay plate which was placed into the pressure vessel and then sealed. At last, the internal pressure was adjusted to the predetermined value.

(3) The discharged water was weighed, then the mass of the sample was determined until the sample inside reached a balanced state while the suction decreased to 0 kPa.

(4) The sample was stressed at a pressure of 0 kPa, 20 kPa, 50 kPa, 100 kPa, 150 kPa, 200 kPa and 350 kPa, respectively. Steps ① ∼ ③ were repeated to stress the sample at different pressure levels.

Based on the experimental results, mass water content was transformed into volumetric water content according to Eq. (1) (Dang Jinqian and Li Fahu, 2013).

$$\theta_w = \left(\rho_d / \rho_w \right) \cdot \omega \tag{1}$$

where ρ_d and ρ_w are maximum soil dry density and water density, respectively. θ_w and ω are the volumetric water content and mass water content, respectively.

RESULTS AND DISCUSSION

Relationship between Dry Density and Fractal Dimension of the Soil Water Characteristic Curve Volumetric Porousity

The internal structure of the soil can significantly influence the SWCC. Therefore, the SWCC and the fractal dimension are connected with fractal theories. In other words, water retention capacity of the soil can be reflected by fractal dimension. Tao et al. (2014) established a fractal model of pore volume in three-dimensional coordinates based on the density distribution function of the pore volume (Katz et al., 1985), as shown in Eq. (2).

$$V\left(>r\right)=V_a\left[1-\left(r/L_2\right)^{3-D}\right] \tag{2}$$

where $V(>r)$ is the accumulated pore volume larger than r; V_a is the total pore volume; L_2 is the scale of the study area; D is the fractal dimension.

On the basis of the Young-Laplace theory, the relationship between matric suction (φ) and effective aperture can be determined by Eq. (3)

$$\psi=2T_s\cos\alpha/r \tag{3}$$

where T_s is the water surface tension and a is the contact angle, respectively. When the temperature is determined, the value of $2T_s\cos a$ can be assumed as constant.

Eq. (4) is given by substituting Eq. (2) into Eq. (3).

$$V_a-V\left(>r\right)/V_a=A\psi^{D-3} \tag{4}$$

where V_a is the air volume.

Hypothesizing that the water density is 1 g·cm⁻³, for soil grains with a mass of 1g, the mass water content is $\omega=V(\leq r)$ $V(\leq r)$, representing the cumulative pore volume with a diameter less than r.

Taking the natural logarithm of Eq. (4) and simplifying it, Eq. (5) can be obtained as follows:

$$\ln\left(1/G_s+\omega\right)=-\left(3-D\right)\ln\psi+\ln B \tag{5}$$

where $B=A/\rho_d$. φ is the matric suction. G_s is the specific gravity. A is the cross-sectional area.

Referring to Eq. (5), it can be seen that the pore fractal dimension is confirmed by the slope of the scatter plot with X-axis of $\ln\psi$ and Y-axis of $\ln(1/G_s+\omega)$. According to the fractal theory, the fractal dimension is 3-k when the data points are linear in two-dimensional coordinates, where the value k is the slope of the line.

Fig. 4 shows the linear relationship between $-\ln\psi$ and $\ln(1/G_s+\omega)$. This suggests that the fractal behavior exists between the mass water content and the matric suction. Meanwhile, the internal pore characteristics of black soil are also reflected by the fractal dimension. The fractal dimension represents the difference of soil grains in size, which ranges from 0 to 3 (Posadas et al., 2001). Higher fractal dimension indicates more uneven soil grains. Particularly, the fractal dimension is 0 when the soil is composed of fixed-size grains. The slope and the fractal dimension are obtained by the fitted data, as shown in Table 1. So, it is obvious that dry density significantly affects the slope and the fractal dimension.

Table 1. The fractal dimension of black soil of different dry densities

Dry density/g·cm⁻³	Fractal dimension D	Dry density /g·cm⁻³	Fractal dimension D
1.45	2.9304	1.65	2.9574
1.50	2.9362	1.70	2.9624
1.55	2.9465		

Based on the least square method, the relationship between fractal dimension and dry density is given as shown in Eq. (6) and can be expressed by a linear

function when the dry density ranges from 1.40 g·cm⁻³ to 1.70 g·cm⁻³. With the increase of dry density, the contact area of soil grains increased. Moreover, the soil

grains are squeezed in all directions and the soil grains become more uniform simultaneously, so that the fractal dimension increases gradually.

$$D = 2.782\rho_{\mathrm{d}} + 0.106 \tag{6}$$
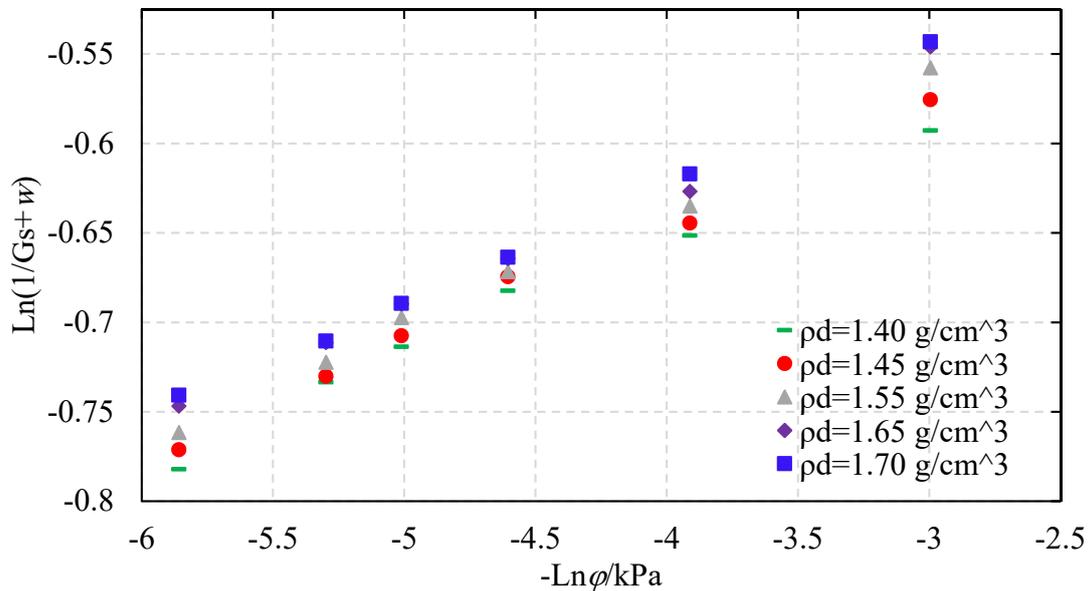
where D is the fractal dimension.

Figure (4): Relationship between parameters -lnψ and ln $(1/G_s+\omega)$

Statistical Model of the Unsaturated Soil Permeability Coefficient

Childs & Collos-George (1950) proposed a mathematical model to evaluate the permeability coefficient of unsaturated soil. After that, the final model was determined on the basis of the improvement and simplification by many researchers (Kunze et al., 1968; Marshall, 1958). The permeability coefficient of mine tailings was calculated by using this model and good accuracy was confirmed. The calculation steps are as follows (Mcqueen et al., 1974; Fredlund et al., 1993). Firstly, the SWCC is divided into m sections on average along the axis of volumetric water content, as shown in Fig. 5. Next, the permeability coefficient $k_w(\theta_w)$ was calculated by using the matric suction of every midpoint of the adjacent section on the basis of Eq. (7) and Eq. (8), respectively

$$k_w\left(\theta_w\right)_i = \frac{k_s}{k_{sc}} A_d \sum_{j=i}^{m}\left[\left(2j+1-2i\right)\psi_j^{-2}\right] \quad \mathrm{j}=1,2,3\cdots\cdots m \tag{7}$$

$$\left. \begin{array}{c} A_{\mathrm{d}} = \dfrac{T_S^2 \rho_W g}{2\mu_w} \dfrac{\theta_s^p}{N^2} \\[2mm] k_{sc} = A_d \sum_{j=i}^{m}\left[\left(2j+1-2i\right)\psi_j^{-2}\right] \quad i=0,1,2,\cdots\cdots m \\[2mm] N = m\dfrac{\theta_s}{\theta_s - \theta_r} \end{array} \right\} \tag{8}$$

where $k_w(\theta_w)$ and m are the permeability coefficient and the midpoint of the adjacent two points, respectively. k_{sc} is the computational saturated permeability and i is the serial number of the discontinuity point. The value of j ranges from i to m.
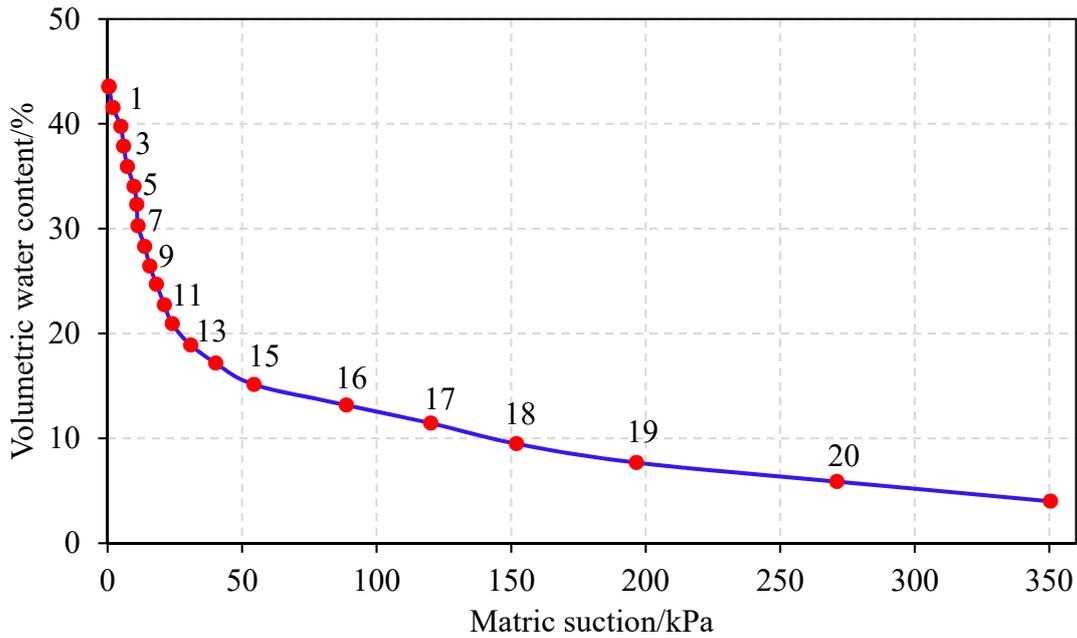
The relative parameters are shown in Table 2.

Figure (5): Schematic diagram of the modified Childs & Collis-George model (Childs et al., 1950)

Table 2. Nomenclature of the modified Childs & Collis-George model (Childs et al., 1950)

Nomenclature	Physical significance	Value	Unit
T_s	water surface tension	7.28×10^{-5}	$kN \cdot m^{-1}$
ρ_w	water density	1.0×10^{3}	$kg \cdot m^{-3}$
g	gravitational acceleration	9.8	$m \cdot s^{-2}$
μ_w	absolute water viscosity	100.5×10^{-5}	$N \cdot m \cdot s^{-2}$
P	constant	2	/
N	total number of breaks between θ_r and θ_s	24	/
A_d	adjustment coefficient	1	/

Table 3. The permeability coefficient of black soil of different matric suction values

Matric suction /kPa	Permeability coefficient $k_w(\theta_w)/m \cdot s^{-1}$	Matric suction /kPa	Permeability coefficient $k_w(\theta_w)/m \cdot s^{-1}$	Matric Suction /kPa	Permeability coefficient $k_w(\theta_w)/m \cdot s^{-1}$
4.7016	1.8695×10^{-6}	11.9349	1.1790×10^{-7}	46.2930	2.0961×10^{-9}
5.7866	1.0499×10^{-6}	14.1049	7.7295×10^{-8}	70.8861	1.0190×10^{-9}
7.9566	7.2241×10^{-7}	16.2749	4.8759×10^{-8}	103.7975	5.0486×10^{-10}
9.7648	5.0354×10^{-7}	18.8065	2.9245×10^{-8}	135.2622	2.2487×10^{-10}
10.4882	3.5847×10^{-7}	22.0615	1.6517×10^{-8}	173.2369	7.9242×10^{-11}
11.9349	2.5455×10^{-7}	26.7631	8.7321×10^{-9}	232.9114	1.6110×10^{-11}
14.1049	1.7547×10^{-7}	34.3580	4.3575×10^{-9}		

k_{sc} equals 1.58 $m \cdot s^{-1}$ based on Eq. (8). Therefore, k_s/k_{sc} is 1.18×10^{-6}, which is utilized to calculate the permeability coefficient of black soil. Then, the dry density value of 1.45 $g \cdot cm^{-3}$ is selected as an example to

calculate the permeability coefficient for different matric suction values. The results are listed in Table 3. The permeability coefficient of black soil decreases with increasing the matric suction because of the varied water content. According to Fig. 4, it is obvious that the smaller the matric suction is, the greater the volumetric water content will be. In the case of high water content, the water is more easily discharged, which means that very weak matric suction can make water flows. Thus, the permeability coefficient is large when the matric suction is weak.

Evaluation of the Applicability of SWCC Model

The SWCC is a key factor to determine the property changes of the soil, which is strongly correlated with numerous factors as aforementioned. For this reason, many models were proposed to obtain the SWCC (Hong et al., 2016; Scanziani et al., 2017; Gardner, 1958). In this paper, the performance of the three SWCC models on black soil was analyzed. The formulae and the relative parameters of the models are as shown in Table 4.

Table 4. Common soil water characteristic curve models

Model	Formula	Descriptions
Fredlund & Xing model (Fredlund, 1994)	$\theta_w = \dfrac{\theta_s}{\left\{\ln\left[e+\left(\dfrac{\varphi}{a}\right)^b\right]\right\}^c}$	θ_w, θ_s and θ_r are volumetric moisture content, saturated volumetric water content and residual volumetric moisture content, respectively, %；ψ is the matric suction, kPa；a, b and c are model parameters, respectively.
Van Genuchten model (Van Genuchten, 1980)	$\theta_w = \theta_r + \dfrac{\theta_s - \theta_r}{[1+(a\varphi)^b]^{1-\frac{1}{b}}}$	
Gardner model (Gardner, 1958)	$\theta_w = \theta_r + \dfrac{\theta_s - \theta_r}{1+a\varphi^b}$	

Analysis of Calculation Results of SWCC Model

Fig. 6 (a) shows the relationship between the matrix suction and the volumetric water content of different dry densities. Both shape and height of SWCC are obviously affected by dry density. In general, the height of SWCC increases with increasing dry density, indicating that dry density significantly affects the holding water capacity of black soil. However, this phenomenon is contrary to the situation when the value of matric suction is less than 25 kPa. Meanwhile, when the matric suction is consistent, the larger the dry density is, the smaller the voids in the soil will be. That stems from the fact that when the soil connectivity worsens, this leads to slower drainage velocity. Therefore, the volumetric water content highly changes. Nevertheless, when the matric suction is small, the initial water content (including the

volumetric water content and the mass water content) decreases with increasing dry density.

As presented in Fig. 6 (b), both saturated water content and residual water content are dramatically affected by dry density. Dry density influences the water content mainly by changing the volume of the pores. As dry density increases, the soil grains occupy more space. In that case, a small quantity of water can make the sample saturated, thus the saturated water content changes a little, but the residual water content decreases with increasing dry density. The higher the dry density is, the steadier the structure of the soil grains will be, which leads to less water evaporation when drying the soil.
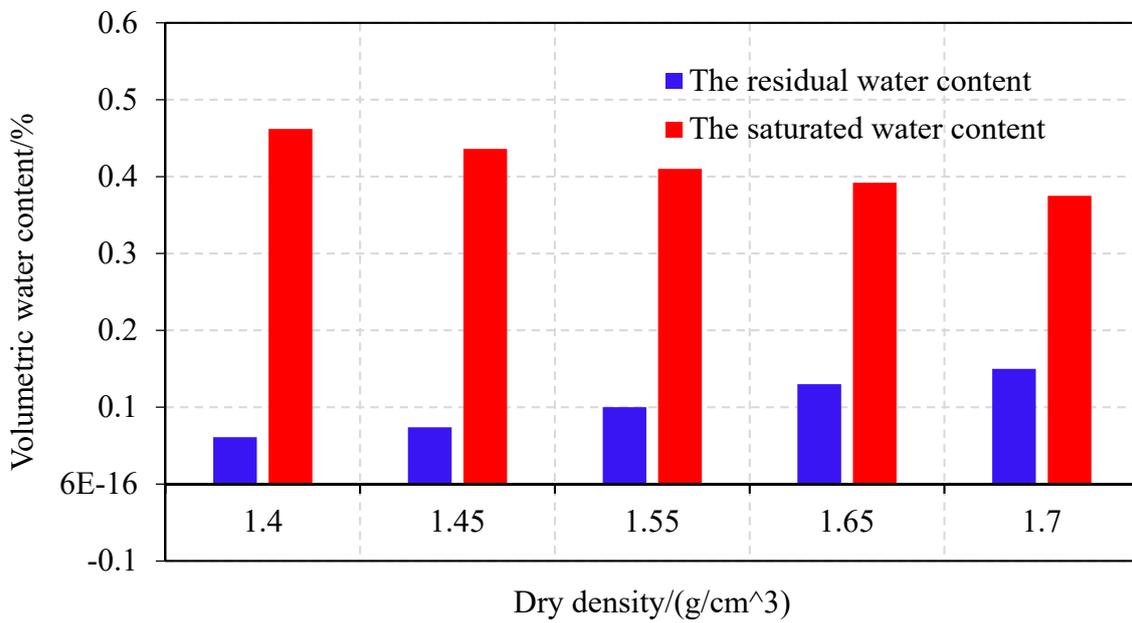
The SWCC is fitted for different dry densities based on the three models. The results and the fitted

parameters are listed in Fig. 7 and Table 5, respectively. All of the decision coefficients (R^2) are larger than 0.96,

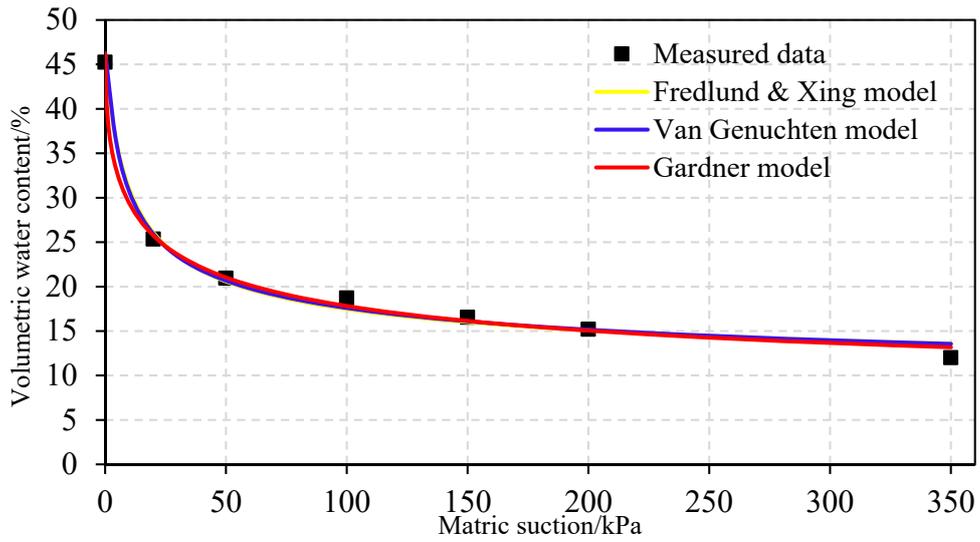indicating that every model could precisely predict the SWCC of black soil.
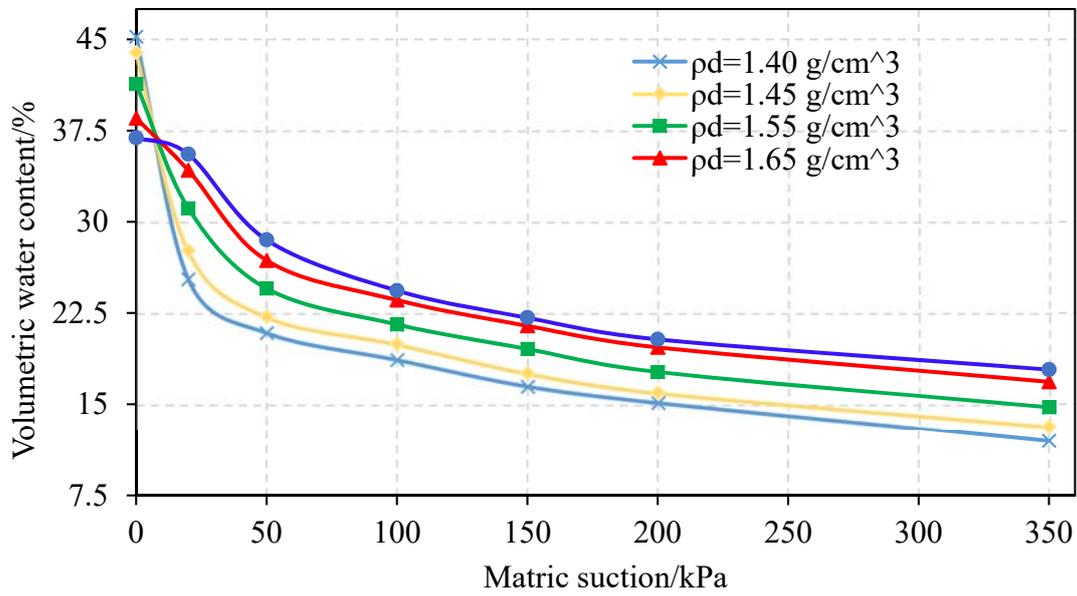
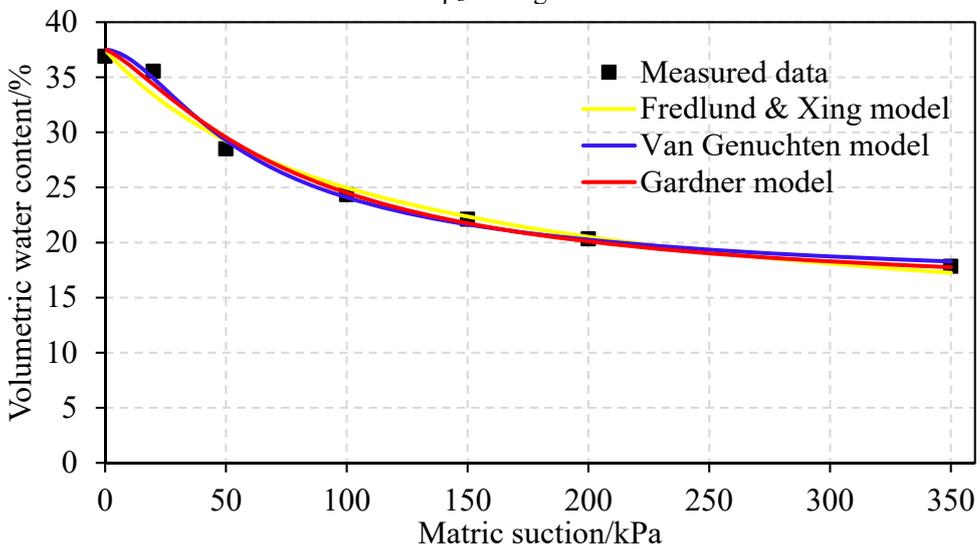(a) The variation in soil water characteristic curve

(b) The variation between saturated and residual water contents
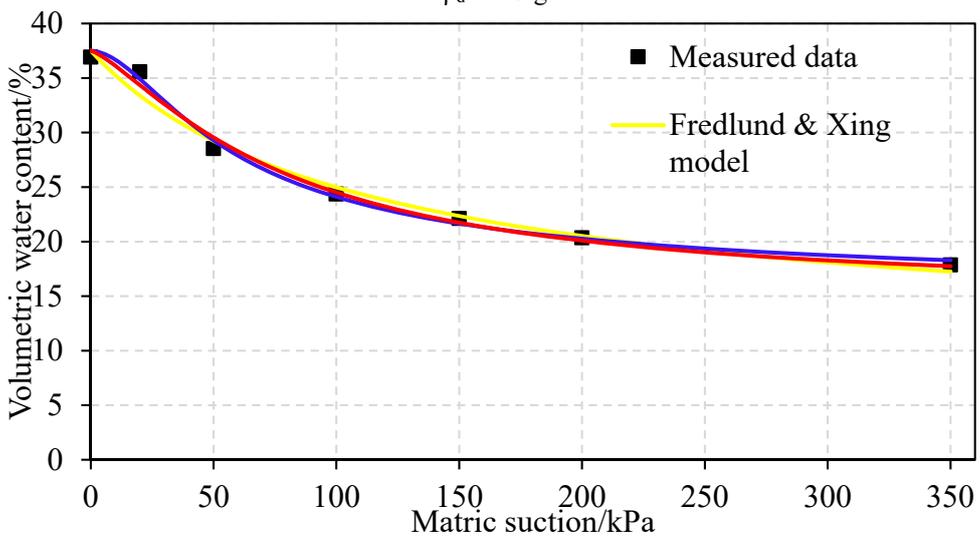
Figure (6): Experimental results of black soil of different dry densities
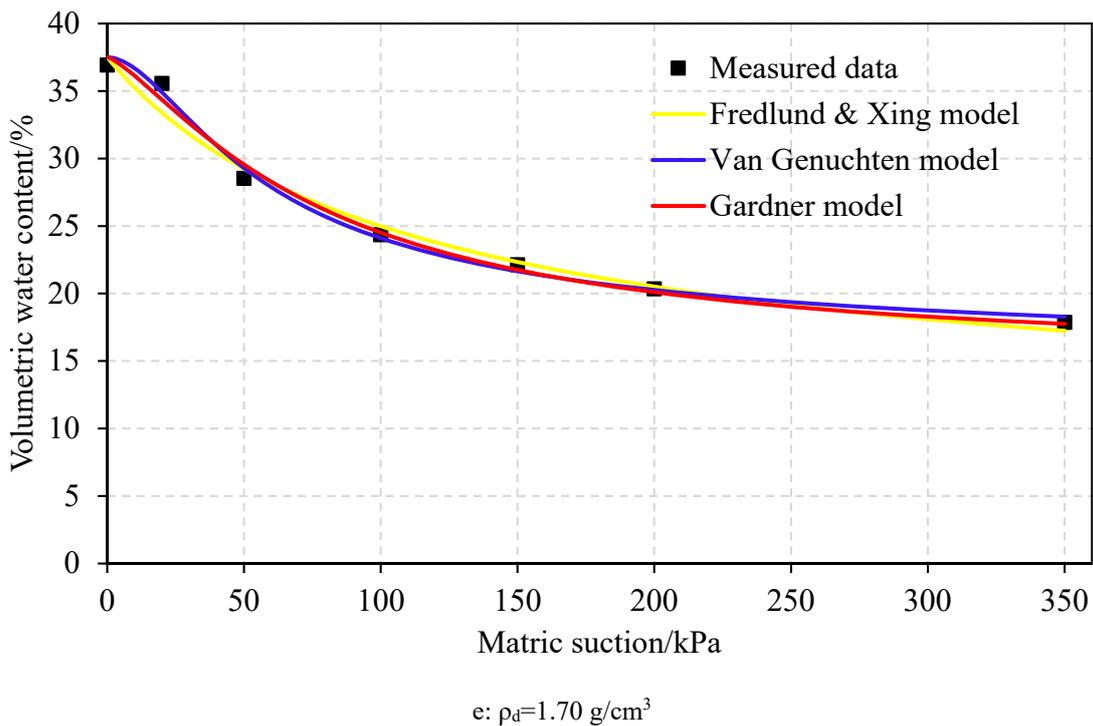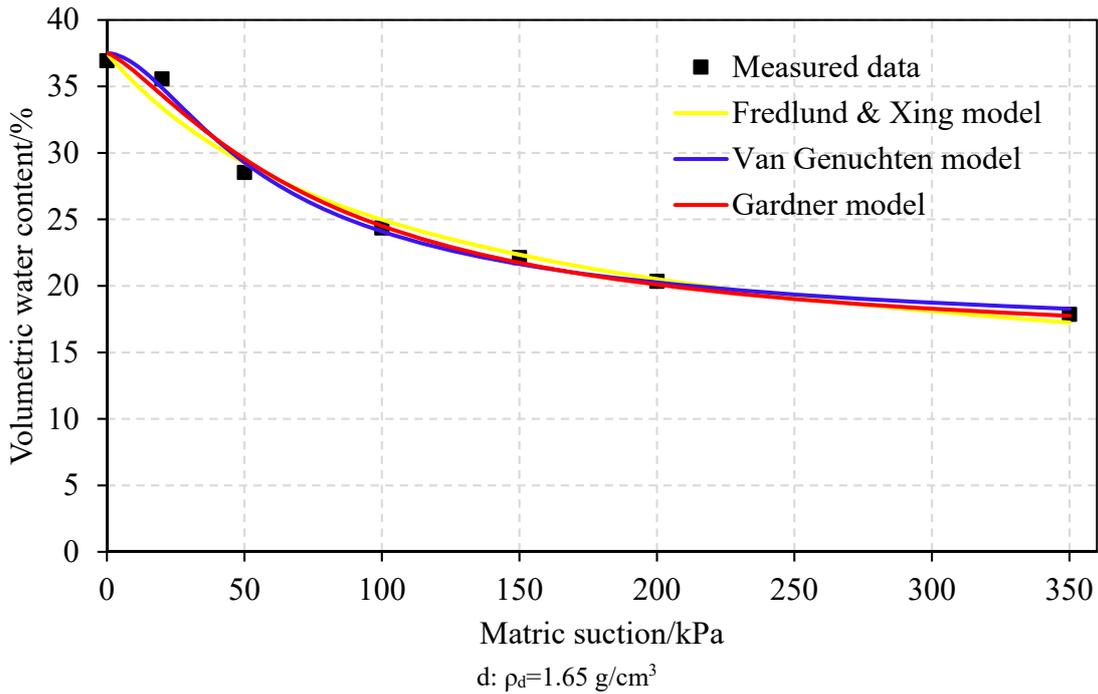
a: ρ_d=1.40 g/cm^3

b: ρ_d=1.45 g/cm^3

c: ρ_d=1.55 g/cm^3

d: ρ_d=1.65 g/cm^3

e: ρ_d=1.70 g/cm^3

Figure (7): Comparison between measured and modeled soil water characteristic curves

From Fig. 7 and Table 5, it is obvious that residual water content, saturated water content and parameters *a*, *b* and *c* are related to dry density, but the effect of dry density on SWCC was not taken into consideration in the equations. Also, it needs to be emphasized that the parameters of the models are complicated and time-consuming to measure in the laboratory, especially for the residual water content.

Moreover, the van Genuchten model (Van Genuchten, 1980) can describe a wider range of water content than Fredlund & Xing model and Gardner model because of its continuity based on previous literature

(Xiao et al., 2007). Therefore, we attempted to optimize the van Genuchten model.

Optimization of van Genuchten Model Based on the Influence of Dry Density

Based on the fitted parameters of the van Genuchten model (Van Genuchtten, 1980), the relationships between dry density and residual water content, saturated water content and parameters a and b are established, respectively. These relationships are as in Eq. (9)～Eq. (12).

$$\theta_r = a_1 + b_1 \rho_d \tag{9}$$

$$\theta_s = c_1 + d_1 \rho_d \tag{10}$$

$$a = e_1 + f_1 \rho_d^{i_1} \tag{11}$$

$$b = h_1^{\rho_d} \tag{12}$$

The fitted parameters are shown in Eq. (13)~Eq. (16). The decision coefficients R^2 are larger than 0.97, indicating that the fitted results are acceptable.

$$\theta_r = -0.3489 + 0.2915 \rho_d \qquad R^2 = 0.99 \tag{13}$$

$$\theta_s = 0.8311 - 0.2685 \rho_d \qquad R^2 = 0.97 \tag{14}$$

$$a = 0.3325 + 1.9122 \times 10^{-4} \rho_d^{14.8915} \qquad R^2 = 0.97 \tag{15}$$

$$b = 24.1266^{\rho_d} \qquad R^2 = 0.98 \tag{16}$$

Replacing θ_r, θ_s and a, b in Eq. (13)~Eq. (16) leads to obtain Eq. (17).

$$\theta_w(\rho_d, \; \varphi) = \theta_r + \frac{\theta_s - \theta_r}{\left(1 + (a\varphi)^b\right)^{1 - \frac{1}{b}}} \tag{17}$$

Based on Eq. (17), the SWCC can be determined by using matric suction and dry density as independent variables. In order to verify the new model's feasibility, the dry density value of 1.45 g·cm⁻³ is taken as an example to calculate the SWCC. The results are presented in Fig. 8. It is clear that the new model has a good predictive capability at different dry densities. The absolute value of the relative error (ARE) for the measured values and calculated values of different matric suction values is shown in Table 6. It is fairly clear that the values are within 6 % except for the matric suction of 350 kPa, (when the matric suction was 350 kPa, the value was 14.56%). The average ARE of different matric suction conditions is 4.50 %.
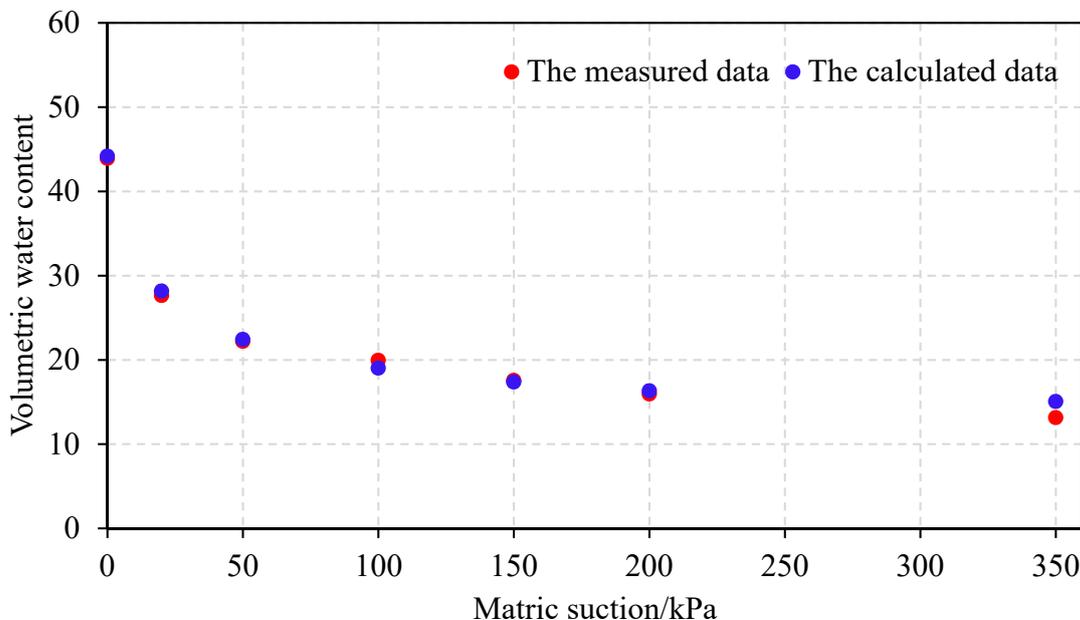

Figure (8): Comparison between the measured soil water characteristic curve and that calculated using the optimized van Genuchten model for the case of (ρ_d=1.45 g/cm³)

Table 6. The absolute value of the relative error for the optimized van Genuchten model used to fit measured data points

Matric suction* (kPa)	0	20	50	100	150	200	350
Absolute value of the relative error	0.58 %	1.93 %	1.02 %	4.70 %	1.06 %	2.40 %	14.56 %

* The dependent variable: volumetric water content

To compare the influence of various parameters on the volumetric water content, the test of subject effect was carried out on matric suction and dry density (the test was not carried out on the parameters a, b, θ_r, θ_s, because these parameters are associated with dry density). As can be seen from Table 7, the effect of dry density on the volumetric water content is greater than that of matric suction.

Table 7. Analysis of the influence of matric suction and dry density on the volumetric water content

Source	Sum of squares	df	Mean square	F	Sig.
Matric suction	2443.19	6	407.20	65.114	.000
Dry density	102.56	4	25.64	4.100	.011
Error	150.87	24	6.25		
Summary	23418.92	35			

CONCLUSIONS

Fractal dimension increases with increasing dry density and the unsaturated permeability coefficient of black soil becomes smaller with the increase in matric suction.

Residual water content increases with increasing dry density. However, the variation regularity of saturated water content is opposite to that of residual water content. When the matric suction is strong, the water content is positively proportional to dry density. But, when the matric suction is weak, the water content is negatively proportional to dry density.

Experimental results indicate that Fredlund & Xing model, van Genuchten model and Gardner model can be used to calculate the SWCC of black soil. Compared with these three models, the optimized van Genuchten model is more qualified for predicting the SWCC of black soil. The ARE decreased from 4.50% to 3.75% at different matric suction values for the dry density value

of 1.45 g·cm⁻³. In addition, the effect of dry density on the volumetric water content is greater than that of the matric suction.

REFERENCES

Alexandra, K., and Zhang, R.D. (1998). "Estimating, the soil water retention from particle-size distributions: a fractal approach". Soil Science,163, 171-179.

Al-Mahbashi, M., T.Y. Elkady, and M.A. Al-Shamrani. (2016). "Hysteresis soil-water characteristic curves of highly expansive clay". European Journal of Environmental & Civil Engineering, 22, 1041-1059.

Arya, L. M., and J. F. Paris. (1981). "A physicoempirical model to predict soil moisture characteristics from particle-size distribution and bulk density data". Soil Science Society of America Journal, 45, 1023-1030.

Arya, L.M., J.L. Heitman., B.B. Tapa, and D.C. Bowman. (2010). "Predicting saturated hydraulic conductivity of golf course sands from particle-size distribution." Soil Science Society of America Journal, 74, 33-37.

Bao, C.G., and L.T. Zhan. (2006). "Relationship between unsaturated soil behavior and engineering problems". Chinese Geotechnical Journal-Engineering, 28, 129-136.

Chen, X., K. Hu, J. Chen, and W. Y. Zhang. (2017). "Laboratory investigation of the effect of initial dry density and grain size distribution on soil–water characteristic curves of wide-grading gravelly soil". Geotechnical and Geological Engineering, 36, 885-896.

Childs, E.C., and G. N. Collis-George. (1950). "The permeability of porous materials". Proceedings of the Royal Society of London.

CMA. (2019). "National meteorological data service center". CMDC.com. Monthly China's surface climate, 1 Jan. 2019. Website.

Corey, A.T., and Brooks, R.H. (1975). "Drainage characteristics of soils". Soil Science Society of America Journal, 39, 251-255.

Dang Jinqian, and Li Fahu. (2013). "Soil mechanics". Beijing: China Water Conservancy and Hydropower Press (in Chinese).

Dong, X., B.P. Singh., G. Li., and Q. M. Lin. (2019). "Biochar increased field soil inorganic carbon content five years after application". Soil & Tillage Research, 186, 36-41.

Elkady, T.Y., A. Al-Mahbashi, M. Dafalla, and M. Al-Shamrani. (2017). "Effect of compaction state on the soil water characteristic curves of sand–natural expansive clay mixtures". Revue Française De Génie Civil, 21, 289-302.

Feng, J., X.Y. Wu, and S.W. Meng. (2017). "Study on the fractal characteristics of soil water characteristic curves of unsaturated clay soil". Journal of Railway Science & Engineering, 14, 1435-1447 (in Chinese).

Fredlund, D.G., A. Q. Xing, and S. Y. Huang. (1994). "Predicting the permeability for unsaturated soils using the soil-water characteristic curve." Canadian Geotechnical Journal, 31, 533-546.

Fredlund, D.G., and H. Rahardjo. (1993). "Soil mechanics for unsaturated soils". Wiley.

Gao, L., Y. C. Tao, L.W. Kong, H. L. Xiao, and Q.S. Chen. (2018). "A simple fractal-based model for soil-water characteristic curves incorporating effects of initial void ratios". Energies, 11, 1401-1419.

Gao, Y., and D.A. Sun. (2017). "Determination of basic parameters of unimodal and bimodal soil water characteristic curves". Chinese Journal of Geotechncial Engineering, 39, 1884-1891.

Gardner, W.R. (1958). "Some steady-state solutions of the moisture flow equations with application to evaporation from a water table". Soil Science, 85, 228-232.

Han, Z.S., and K. Vanapalli. (2016). "Stiffness and shear strength of unsaturated soils in relation to soil-water characteristic curve". Géotechnique, 66, 627-647.

Hong, W. T., Y. S. Jung, S. Kang, and J. S. Lee. (2016). "Estimation of soil-water characteristic curves in multiple-cycles using membrane and TDR System". Materials, 9, 1019-1034.

Jiang, Y., Chen, W.W., G.H. Wang, and G.P. Sun. (2016). "Influence of initial dry density and water content on the soil-water characteristic curve and suction stress of a reconstituted loess soil". Bulletin of Engineering Geology and the Environment, 76, 1085-1095.

Katz, J., and A.H. Thompson. (1985). "Fractal sandstone pores: implications for conductivity and pore formation". Physical Review Letters, 54, 1325-1328.

Kunze, R.J., G. Uehara, and K. Graham. (1968). "Factors important in the calculation of hydraulic conductivity". Soil Science Society of America Journal, 32, 760-765.

Li, J.H., Z. Lu, L. B. Guo, and L. M. Zhang. (2017). "Experimental study on soil-water characteristic curve for silty clay with desiccation cracks". Engineering Geology, 218, 70-76.

Liu, W. P., X. Y. Luo, and F. M. Huang. (2017). "Uncertainty of the soil-water characteristic curve and its effects on slope seepage and stability analysis under conditions of rainfall using the markov chain Monte Carlo method". Water, 10, 1-17.

Marshall, T.J. (1958). "A relation between permeability and size distribution of pores". European Journal of Environmental & Civil Engineering, 9, 1-8.

Mcqueen, S., and R.F. Miller. (1974). "Approximating soil moisture characteristics from limited data: empirical evidence and tentative model". Water Research ,10, 521-527.

Mill, C. J. (2002). "Impact of soil type and compaction conditions on soil water characteristics". Journal of Geotechnical and Geoenvironmental Engineering, 128, 733-742.

Minh, T. K., and A. Mahler. (2018). "A study on the relationship between matric suction and the void ratio and moisture content of a compacted unsaturated soil". Periodica Polytechnica Civil Engineering, 62, 709-716.

Ministry of Water Resources of the People's Republic of China. (2019). "Chinese standard for soil test method". China Planning Press, Beijing (in Chinese).

Omer Muhie Eldeen Taha and Moh'd Raihan Taha. (2015). "Volume change and hydraulic conductivity of soil-bentonite mixture". Jordan Journal of Civil Engineering, 9 (1), 43-58.

Philip, J.R., and D.A. De Vries. (1957). "Moisture movement in porous materials under temperature gradients". Transactions, American Geophysical Union, 38, 222-232.

Posadas, N.D., D. Gime´nez, M. Bittelli, C. M. P. Vaz, and M. Flury. (2001). "Multifractal characterization of soil particle-size distributions". Soil Science Society of America Journal, 65, 1361-1367.

Sahis, M.F., and Biswas, P.P. (2017). "Comparative deterministic and probabilistic analysis of two unsaturated soil slope models after rainfall infiltration". Jordan Journal of Civil Engineering, 11 (1), 142-148.

Scanziani, K. Singh, M. J. Blunt, and A. Guadagnini. (2017). "Automatic method for estimation of in situ effective contact angle from X-ray micro-tomography images of two-phase flow in porous media." Journal of Colloid and Interface Science, 496, 51-59.

Sedano, P.R., and J.I. Sedano. (2016). "Incorporating temperature effects in soil-water characteristic curves". Indian Geotechnical Journal, 46, 309-318.

Shi, J., X. Wu, A.Y., and Z. Zhang. (2018). "Laboratory test investigations on soil water characteristic curve and air permeability of municipal solid waste". Waster Management & Research, 36, 1-8.

Tabana, M., Mirmohammad Sadeghi, and M.A. Rowshanzamirc. (2018). "Estimation of van Genuchten SWCC model for unsaturated sands by means of genetic programming". Scientia Iranica A, 25, 2026-2038.

Tao, G.L., J. R. Zhang, X.S. Zhuang, and L. Yang. (2014). "Influence of compression deformation on the soil-water characteristic curve and its simplified representation method". Journal of Hydraulic Engineering, 45, 1239-1245.

Tao, H., C. Chen, P. Jiang, and Y.T. Li. (2017). "Soil water characteristic curves based on particle analysis." Procedia-Engineering, 174, 1289-1295.

Van Genuchten, M.T. (1980). "A closed form equation for prediction of hydraulic conductivity of unsaturated soils". Soil Science Society of America Journal, 44, 892-898.

Wheatcraft, S.W., and S.W. Tyler. (1988). "An explanation of scale-dependent dispersivity in heterogeneous aquifers using concepts of fractal geometry". Water Resources Research, 24, 566-578.

Xiao, J.Y., Y.T. Li, and L. Wang. (2007). "Fitting soil water characteristic curve based on the van Genuchten model". Goungwater, 29, 46-47.

Zhai, Q., H. Rahardjo, and A. Satyanaga. (2016). "Variability in unsaturated hydraulic properties of residual soil in Singapore". Engineering Geology, 209, 21-29.

Zheng, E., H. Yang., and X. Z. Zhang. (2018). "Influence of different nitrogen forms' application on rice photosynthesis: fluorescence with water-saving irrigation in black soil region of Songnen Plain, Northeast China". Paddy and Water Environment, 16, 795-804.